buildings

MDPI

Article

Study on Application of Transparent Soil in Migration of Heavy Metal Pollutants in Porous Media

Congcong Zhao, Hemiao Yu, Zhenxiao Qi and Min Li *

College of Civil Engineering and Transportation, Hebei University of Technology, Tianjin 300131, China; zhaocc0409@163.com (C.Z.); 18822121979@163.com (H.Y.)
* Correspondence: limin-0409@163.com

Abstract: Clarifying the migration law of heavy metal pollutants in soil is the key prerequisite for its treatment. Because most heavy metal pollutants possess color-rendering properties, it is theoretically feasible to use synthesized transparent soil to simulate the migration and diffusion of heavy pollutants in soil. In order to assess the feasibility of employing transparent soil for investigating heavy metal migration (singly and multiply) in porous media, the fluctuation rates and concentration distribution of pollutants were measured from both vertical and horizontal perspectives. Simultaneously, the effects of temperature, dry density, and initial concentration on heavy metal migration were investigated simultaneously, while analyzing changes in heavy metal occurrence forms during the migration process. The study shows that transparent soil accurately simulated heavy metal migration with a deviation of less than 10% compared to sandy soil. The migration of Cu(II) in a single heavy metal migration test was greatly affected by three factors. Among them, both Cu(II) and Cr(VI) are similarly affected by the initial concentration, and favorable migration occurs at an initial concentration of 1000 mg/kg. The heat source temperature and initial concentration significantly impact the migration of single Cr(VI) and composite heavy metals. Under the influence of heat source temperature, the increase in heavy metal migration rate is associated with an increase in the proportion of exchangeable (EXC) and carbonate-bound (Carb). Studying the interaction mechanism between these factors is crucial for accurately predicting the transport behavior of heavy metal pollutants in porous media and providing a scientific basis for environmental protection and treatment.

Keywords: heavy metal pollution; migration patterns; occurrence forms; porous media; transparent soils

Academic Editors: Md. Safiuddin and Muhammad Junaid Munir

Received: 3 December 2024
Revised: 4 February 2025
Accepted: 14 February 2025
Published: 17 February 2025

Citation: Zhao, C.; Yu, H.; Qi, Z.; Li, M. Study on Application of Transparent Soil in Migration of Heavy Metal Pollutants in Porous Media. *Buildings* **2025**, *15*, 612. https://doi.org/10.3390/buildings15040612

1. Introduction

Heavy metal pollution in soil, as one of the primary forms of environmental pollution worldwide, poses significant threats to environmental quality, human health, and national food security [1,2]. Sources of heavy metal pollutants include dust settling from the atmosphere, irrigation with polluted river water, discharge of solid waste, and so on. After entering the soil environment, these pollutants predominantly contaminate the atmosphere and groundwater through processes such as volatilization, atmospheric deposition, and precipitation. They subsequently enter the human body via the food chain, leading to both direct and indirect harm to human health and ecological development [3,4]. And it comprises lead (Pb), copper (Cu), chromium (Cr), cadmium (Cd), nickel (Ni), etc. [5]. These pollutants can persist in the soil for a long time, and show the characteristics of dispersion, migration, diffusion, and accumulation [6,7]. Therefore, the reasonable treatment of heavy metal pollutants in soil is the key to maintain soil health [8–10].

A preliminary framework for the remediation technology system, encompassing bioremediation, physical remediation, and chemical remediation technologies, was established [11–13]. However, the implementation of large-scale soil remediation work with varying pollution levels remains challenging for the economy and efficiency [14]. Grasping the migration law of heavy metals in soil can accurately predict the pollution range and level and prompt science remediation [9]. The development of transparent soils with properties similar to natural soils has created opportunities for visual research on the internal structure of soils [15,16]. At present, transparent soil has been widely used in the research field of soil hydraulics because of its excellent applicability [17,18]. For instance, transparent soil was employed to investigate the interaction between pile body and surrounding soil during the process of pile formation [19].

Heavy metals exhibit distinct coloration, making it theoretically viable to employ transparent soil to investigate the migration of heavy metal pollutants within soil environments [20]. This study examines the practicality of visually tracking pollutant migration in soil by comparing the movement behaviors of typical heavy metals—Cu(II) and Cr(VI)—as well as their composite pollutants, both in transparent and sandy soils. The research further elucidates the interfacial migration patterns of these pollutants, using the temperature field as a driving force while considering soil density and pollutant concentration as influencing factors. Moreover, the classical Tessier five-step sequential extraction method [21,22] is utilized to determine the distribution of heavy metal concentrations and their forms in both vertical and horizontal directions. The findings from this study will enhance the understanding of contaminant transport in porous media and offer technical guidance for the effective remediation of heavy metal-contaminated soils.

2. Materials and Methods

2.1. Experimental Materials

Compared to natural soil, transparent soil not only exhibits comparable physical and mechanical properties but also achieves visual transparency. Transparent soil primarily consists of two components: solid particles and pore fluids. The solid particles are predominantly composed of fused quartz sand with a particle size ranging from 0.50 to 1.00 mm. Fused quartz sand possesses exceptional chemical stability and mechanical strength, enabling the transparent soil to maintain consistent properties under various experimental conditions. The pore fluid is a 61% calcium bromide ($CaBr_2$) solution, whose refractive index matches that of the solid particles, rendering the entire material transparent. This specialized fluid not only fills the interstitial spaces between particles but also simulates groundwater or liquid flow through the soil without compromising transparency.

For comparative analysis, ISO standard sand with a particle size of 0.50 to 1.00 mm was utilized (see Table 1). ISO standard sand is a widely used reference material in civil engineering and geology, characterized by its strictly controlled particle size and shape to ensure experimental repeatability and reliability. By comparing these two materials, the similarity between transparent soil and sandy soil can be more thoroughly investigated. For instance, permeability tests revealed a high degree of consistency in water penetration rates between transparent soil and ISO standard sand. Additionally, compression tests demonstrated similar stress–strain curves for both materials. These findings indicate that transparent soil not only resembles natural sand in appearance but also exhibits highly similar mechanical behavior [23,24].

Table 1. Main test material.

Materials Name	Specification	Properties
Cupric chloride	Analytically pure	Relative density 3.386 g/cm^3; melting point 620 °C; boiling point 993 °C.
Potassium chromate	Analytically pure	Relative density 2.732 g/cm^3; melting point 971 °C.
Calcium bromide	Analytically pure	Relative density 3.353 g/cm^3; melting point 730 °C; boiling point 806~812 °C.
Fused quartz sand	Particle size 0.5 mm~1.0 mm	SiO_2 99.9~99.95%; True specific gravity: 2.21; mohs hardness: 7.0; pH value: 6.0
China ISO standard sand	Particle size 0.5 mm~1.0 mm	SiO_2 > 95%; fineness modulus 2.3~3.0; density 1.62 g/cm^3.

Copper chloride and potassium chromate were used to provide heavy metal ions of Cu(II) and Cr(VI). Based on the screening values for Cu(II) and Cr(VI) in the current soil pollution risk control standards for agricultural land (GB15618-2018), the contaminated concentrations were established at 500, 1000, and 1500 mg/kg (on a dry soil mass basis). The ratios of composite ions Cu(II) to Cr(VI) in the resulting heavy metal-contaminated soil were set at 1:1, 4:6, and 6:4, respectively. Furthermore, in the experimental design, three parallel experimental groups were established for each condition to ensure the accuracy and rigor of the test data.

2.2. Testing Apparatus

A self-constructed testing apparatus was employed to conduct the experiment, as depicted in Figure 1a. The apparatus is fabricated from organic glass material, with internal dimensions measuring 70 mm in diameter and 140 mm in height, and with the help of a constant temperature water bath and heat-proof material to achieve temperature control of 20 °C, 40 °C, 50 °C, and 60 °C, respectively. The specimen was divided into eight sections (labeled as I, II ~ VIII) with a 20 mm interval from top to bottom, as illustrated in Figure 1b.

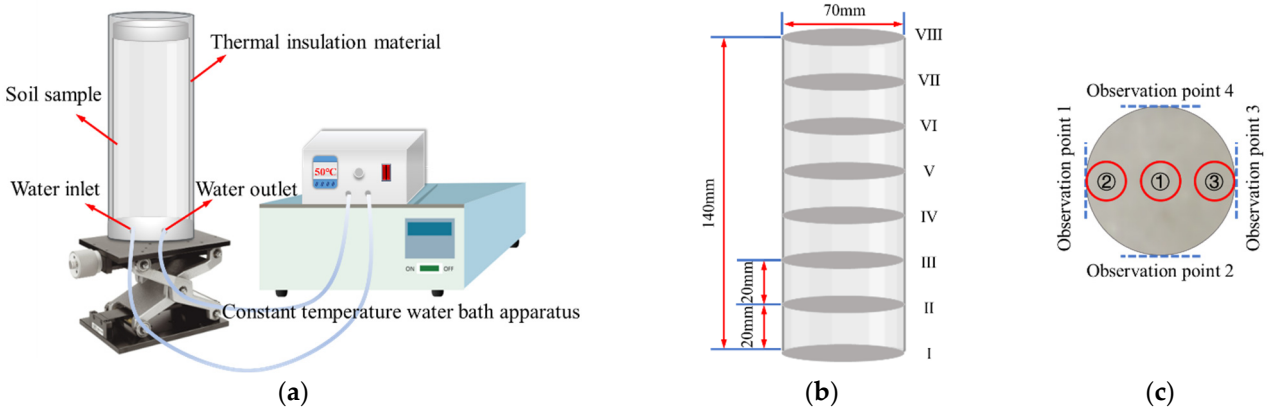

Figure 1. Schematic diagram of test device. (**a**) Test device. (**b**) Sample division. (**c**) Observation points.

In the experiment, four key observation points were measured every 20 min to record the migration distance of the heavy metal pollutants (Figure 1c). These observation points were strategically placed to cover critical locations within the experimental area, thereby reflecting the overall migration trend of the pollutants. When the migration distance stabilizes, it indicates that the diffusion rate has slowed down or reached equilibrium. At this stage, three sampling points were established along the axial direction of each section to ensure a comprehensive representation of pollutant concentration changes within the area. Each sampling point was sampled three times per trial to minimize random errors and

enhance data reliability. All samples were immediately labeled, stored, and transported to the laboratory for analysis.

2.3. Sample Preparation

2.3.1. Transparent Soil Sample

Molten quartz sand was first rinsed with deionized water and dried. And then, the molten quartz sand was slowly added to the calcium bromide solution by stirring with a glass rod. After thorough mixing, the mixture was placed in a dark environment for one hour. The transparent soil prepared can clearly show the grid below the beaker (Figure 2).

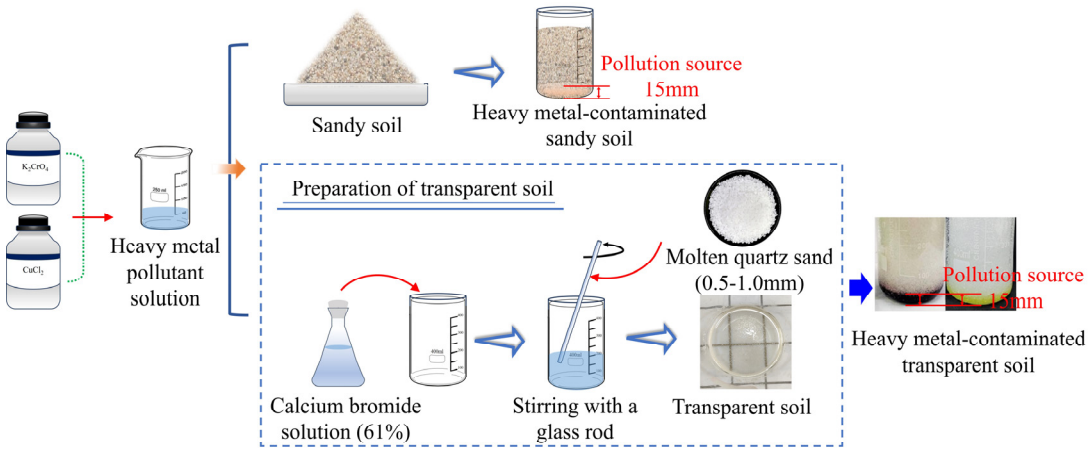

Figure 2. Sample preparation flow chart.

2.3.2. Heavy Metal-Contaminated Soil Sample

The required masses of copper chloride and potassium chromate were accurately weighed based on the predetermined pollution concentration values, then dissolved in a precisely measured volume of distilled water (19.4% moisture content for transparent and sandy soils). A known mass of dry and clean test soil was quantitatively weighed and placed into a container. The pollutant solution was added to the soil, which was then thoroughly mixed and stirred. The mixture was subsequently wrapped with plastic film and allowed to stand for 12 h. Following this, the heavy metal-contaminated soil was compacted using a hammer to form a 15 mm high pollution source at the high-temperature heat source end (Figure 2). The dry densities of the prepared soils were 1.3, 1.4, and 1.5 g/cm^3, respectively.

2.4. Index Test Methods

The concentrations of Cu(II) and Cr(VI) were quantified using a Skyray EDX series energy dispersive spectrometer. The detection limits for Cu(II) and Cr(VI) are 0.04 mg/kg and 0.10 mg/kg, respectively, with pure SiO_2 serving as the test substrate. The samples were placed in aluminum foil containers, dried at 105 °C, and subsequently ground into a 2 mm powder for analysis. Each measurement was conducted for 100 s, and the average of three replicate measurements was used to determine the final concentration values.

Additionally, the Tessier sequential extraction method is currently widely employed for the speciation analysis of heavy metal (exchangeable (EXC), carbonate-bound (Carb), Fe-Mn oxides bound (FeMnOx), organic matter/sulfide-bound (OM), and residual (RES)) [25]. On this basis, Rauaret et al. [26] refined the Tessier continuous extraction method. In conjunction with the aforementioned literature, this study used a constant temperature shaker, electronic centrifuge, atomic absorption spectrophotometer, and other instruments for the experiments. The procedures for speciating Cu(II) and Cr(VI) are detailed in Table 2.

Table 2. Five-step Tessier sequential extraction method.

Procedure	Form	Reagents and Operation Methods
1	EXC	10 mL 1 mol/L $MgCl_2$, pH = 7.34, shaken at 25 °C for 1 h, centrifuged at 4000 r/min for 5 min, the supernatant was removed and filtered, and the volume was constant in a 50 mL volumetric flask.
2	Carb	10 mL 1 mol/L NaAc, pH = 5.0, shaking at 25 °C for 5 h, centrifugation at 4000 r/min for 5 min, the supernatant was removed and filtered, and the volume was constant in a 50 mL volumetric flask.
3	FeMnOx	20 mL 0.04 mol/L $NH_2OH{\cdot}HCl$, pH = 2, shake at 96 °C for 6 h, centrifuge at 4000 r/min for 5 min, the supernatant was removed and filtered, and the volume was constant in a 50 mL volumetric flask.
4	OM	3 mL 0.02 mol/L HNO_3, 5 mL 30% H_2O_2, shaken at 85 °C for 2 h, added 3 mL 30% H_2O_2, shaken at 83 °C for 3 h, centrifuged at 4000 r/min for 5 min, the supernatant was removed and filtered, and the volume was constant in a 50 mL volumetric flask.
5	RES	The total amount of heavy metals minus the above four forms.

3. Results and Discussion

3.1. Feasibility Analysis of Transparent Soil Application

The feasibility of applying transparent soil to realize the visualization of pollutant migration is evaluated by the fluctuation rate of point concentration difference (Formula (1)).

$$V = \frac{|C_t - C_s|}{C_s} \times 100\% \quad (1)$$

where V is the fluctuation rates, %; C_t is the concentration of heavy metals at a certain point in transparent soil, mg/kg; and C_s is the concentration of heavy metals in the sandy soil, mg/kg.

3.1.1. Comparison of Vertical Migration of Single Heavy Metal

Taking the effects of 1000 mg/kg and 50 °C as an example, the data at the center of each section (point ①) were analyzed. The distribution regularity of Cu(II) and Cr(VI) concentrations in transparent soil and sandy soil is essentially the same at different heat source temperatures and initial heavy metal concentrations (Figure 3). Moreover, it is evident that the concentration distribution curves for the transparent and sandy soils exhibit substantial overlap, indicating a high level of overall agreement between them.

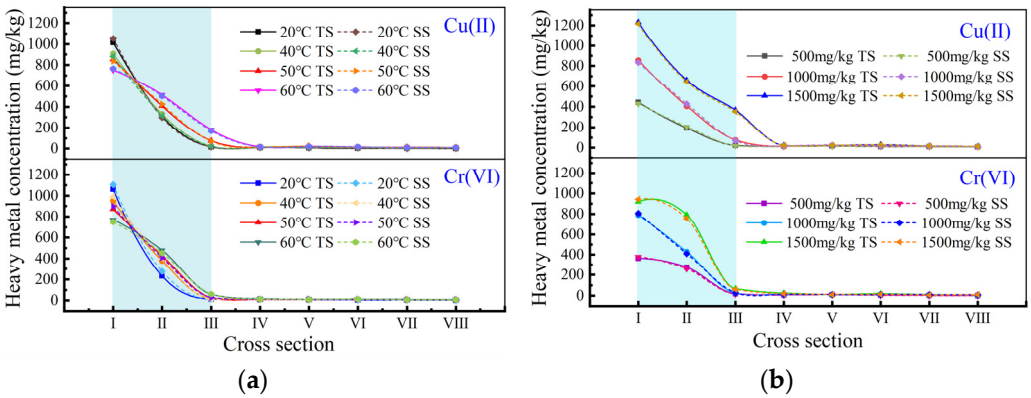

Figure 3. Contaminated soil concentration distribution curves. (**a**) Different heat source temperatures at 1000 mg/kg. (**b**) Different initial heavy metal concentrations at 50 °C.

As the concentration values beyond the section of III approach zero, the fluctuation rate of sections of I, II, and III is analyzed (Figure 4). Under the influence of temperature,

the fluctuation rate at the sections of I, II, and III is below 4%, 6%, and 10%, respectively (Figure 4a). In addition, the distribution with temperature changes from a decreasing pattern at section I to an increasing pattern at sections II and III. It indicates that the increase in temperature can increase the migration of heavy metals. The findings in section III indicate that the impact of temperature on the migration of Cu(II) in soil surpasses that of Cr(VI).

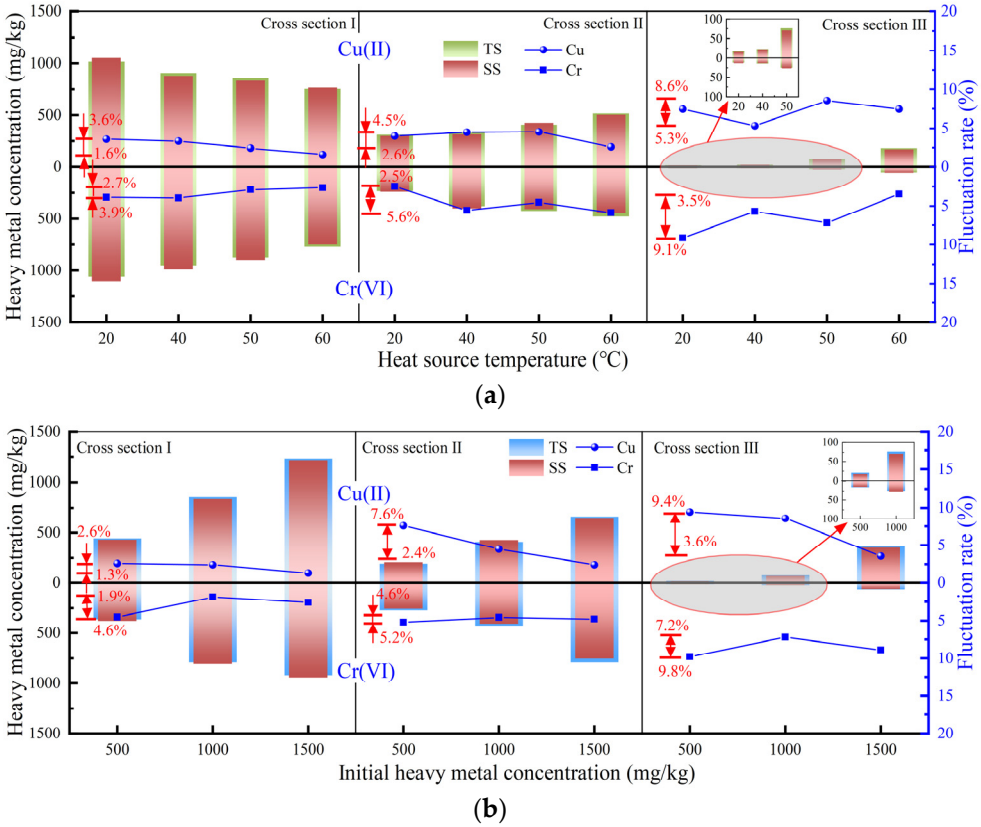

Figure 4. Vertical migration comparison of Cu(II) or Cr(VI) concentrations and fluctuation rates. (**a**) Different heat source temperatures at 1000 mg/kg. (**b**) Different initial heavy metal concentrations at 50 °C.

Under the influence of initial concentrations, the concentration of Cu(II) increases while its fluctuation rate on each profile decreases (Figure 4b). This phenomenon indicates that the simulation effect of transparent soil on sandy soil for Cu(II) intensifies with increasing initial concentrations. Conversely, for Cr(VI), a noticeable rise in fluctuation rate occurs when the initial concentration exceeds 1000 mg/kg, suggesting a slight reduction in the simulation effect of transparent soil on sandy soil at elevated levels of Cr(VI). In section III, the concentration of Cu(II) is higher than that of Cr(VI), indicating that changes in initial concentration have a significant impact on the migration behavior of Cu(II).

3.1.2. Comparison of Lateral Migration of Single Heavy Metal

The concentrations and fluctuation rates of Cu(II) and Cr(VI) lateral migrations were analyzed and compared at points ①, ②, and ③ across various cross sections, as depicted in Figure 5. Under identical conditions, the concentration at the central point of each cross section (point on cross section ①) surpasses that at both sides (points on cross sections ② and ③), for both transparent and sandy soil. This phenomenon becomes more evident as the cross sectional position increases. Furthermore, the fluctuation rate increases with distance from the heat source, but it remains below 10%.

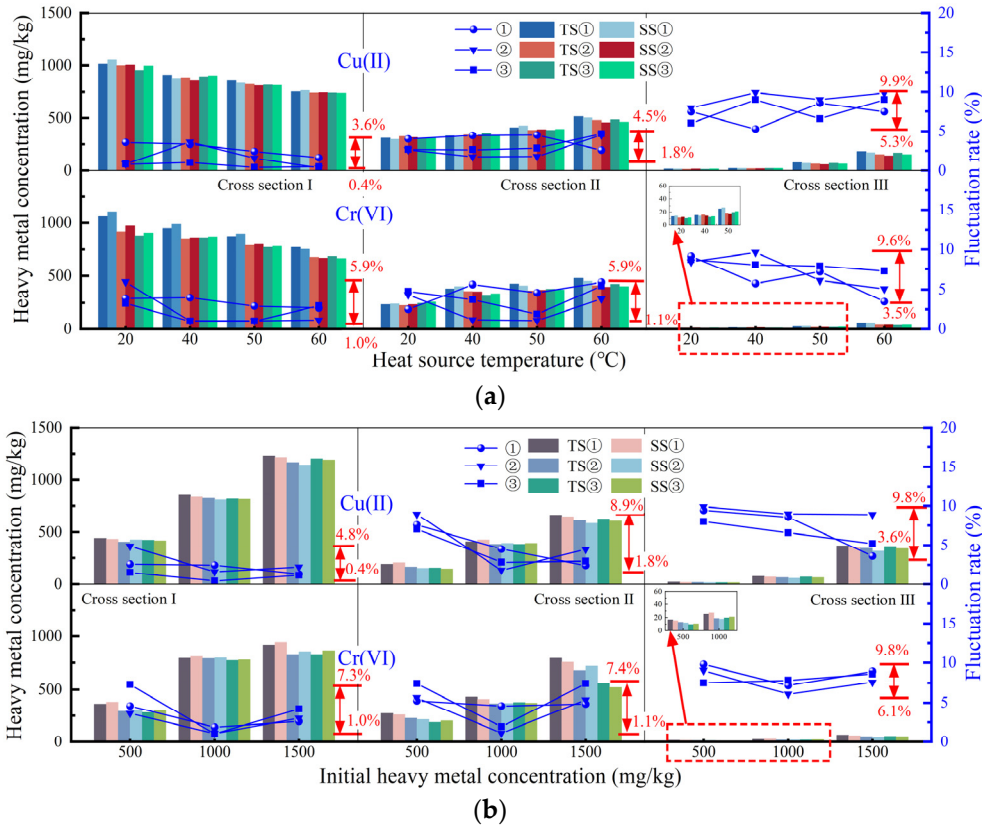

Figure 5. Lateral comparison of concentration distributions and fluctuation rates of Cu(II) and Cr(VI). (**a**) Different heat source temperatures at 1000 mg/kg. (**b**) Different initial heavy metal concentrations at 50 °C.

The fluctuation rate of Cu(II) decreases gradually with increasing initial concentration in the same cross section, similar to the vertical migration law (Figure 5b). Among Cr(VI) pollutants, the fluctuation rate is minimized at an initial concentration of 1000 mg/kg (Figure 5b). Combining these findings with Figures 4 and 5, it can be observed that the influence of heat source temperature and initial concentration of Cu(II) pollutants is more significant compared to Cr(VI) pollutants during both lateral and vertical migration.

3.1.3. Comparison of Migration of Composite Heavy Metals

(1) Vertical migration

Based on the concentration distribution curve of composite heavy metal-contaminated soil, it can be observed that the concentration curves of transparent and sandy soils exhibit a high degree of similarity (Figure 6). This suggests that simulating the vertical migration of Cu(II) and Cr(VI) composite heavy metals in sandy soil using transparent soil is a feasible approach. When the Cu(II) to Cr(VI) ratio is 1:1, the concentration curve of Cr(VI) shows a more gradual change compared to that of Cu(II) (Figure 6b). At a heavy metal concentration of 1500 mg/kg, the difference in Cr(VI) concentration between section II and section I does not exceed 132.23 mg/kg. In contrast, for Cu(II), the concentration difference is at least 397.22 mg/kg. These results indicate that under identical conditions of complex heavy metals, Cr(VI) exhibits better migration than Cu(II). In addition, the influence of temperature on Cu(II) is greater than that of Cr(VI). When the heat source temperature is 40, 50, and 60 °C, the distribution of Cr(VI) exhibits a dense pattern (Figure 6a).

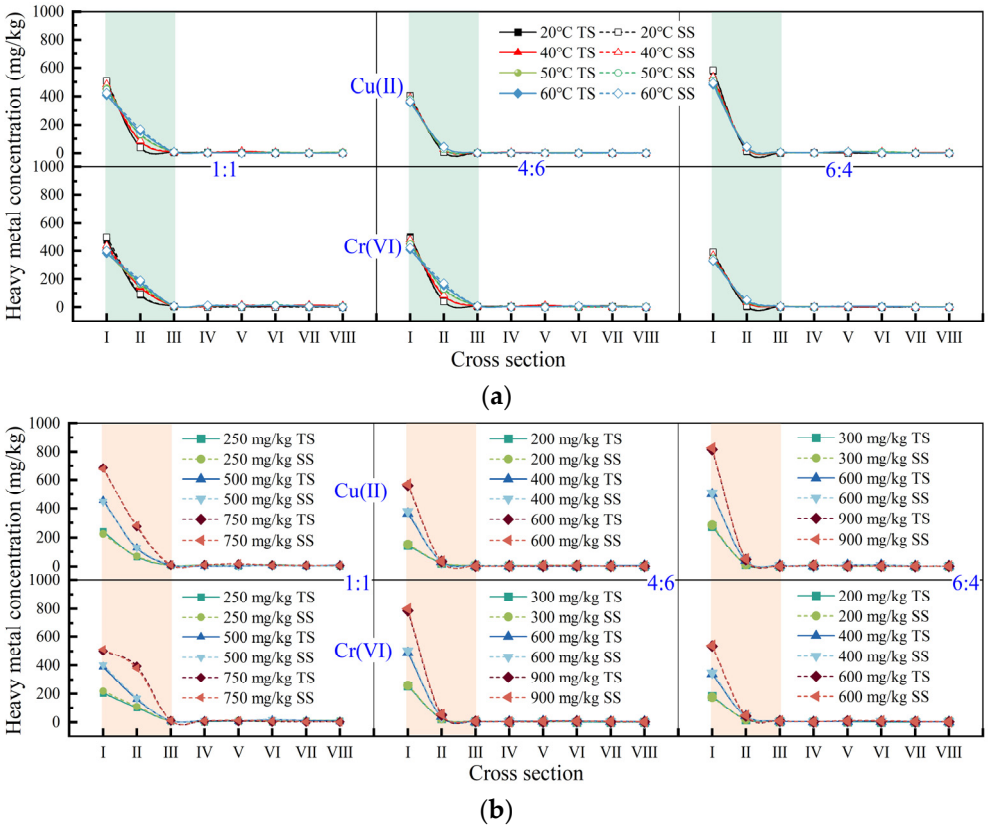

Figure 6. Concentration distribution curves of composite heavy metal-contaminated soil. (**a**) Different heat source temperatures at 1000 mg/kg. (**b**) Different initial heavy metal concentrations at 50 °C.

(2) Lateral migration

The concentration of pollutants approaches zero after section II, so the lateral migration analysis of composite heavy metals is conducted at sections I and II (Figure 6). The migration pattern of complex heavy metal pollutants in soil resembles that of single heavy metals, with accumulation toward the center from both sides (Figure 7). When the ratio of Cu(II) and Cr(VI) is 1:1, both elements exhibit a fluctuation rate below 10%. However, when the ratio becomes 4:6 and the heat source temperature is set at 20 °C, the fluctuation rate of Cu(II) in cross section II exceeds 10% but it is still less than 25% (Figure 7a). The difference in heavy metal concentrations between transparent soil and sandy soil was only 1.37 mg/kg and 1.30 mg/kg under these conditions. The absence of a temperature gradient is considered the main reason for this phenomenon. In section II, heavy metal migration is solely driven by molecular diffusion and mechanical dispersion, resulting in very low concentrations. This further confirms the significant impact of temperature on heavy metal transport in soil. A similar observation can be made from Figure 7b.

When the ratio of Cu(II) to Cr(VI) is 6:4 and the initial concentration of heavy metals is 500 mg/kg, the fluctuation rate of Cr(VI) at the three points in Figure 7d is less than 20% but more than 10%. This is mainly due to the relatively low initial concentration of heavy metals, resulting in lower intermolecular activity compared to other groups. Therefore, despite the temperature gradient influence, a relatively low concentration of heavy metals is still maintained in this section. The results shown in Figure 7 suggest that using transparent soil instead of sandy soil for studying heavy metal pollution achieves over 90% simulation accuracy when the initial concentration of Cu(II) and Cr(VI) composite heavy metals is 1500 mg/kg. Under composite conditions when the ratio of Cu(II) to Cr(VI) is 1:1, simulated transparent soil of sandy soil exhibits optimal performance.

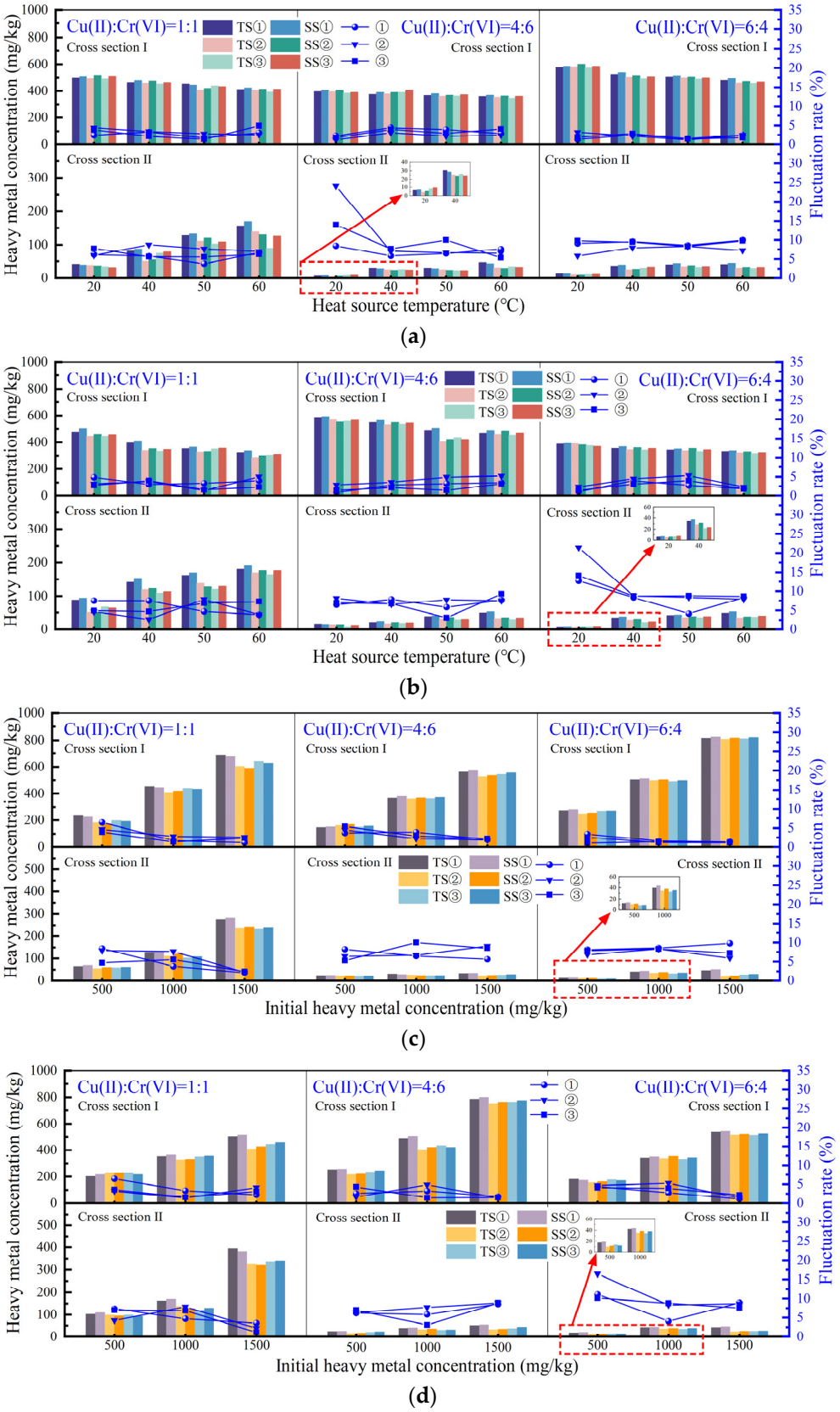

Figure 7. Horizontal comparison of concentration distributions and fluctuation rates of Cu(II) and Cr(VI) composite heavy metal-contaminated soil. (**a**) Cu(II) under different heat source temperatures at 1000 mg/kg. (**b**) Cr(VI) under different heat source temperatures at 1000 mg/kg. (**c**) Cu(II) under different initial heavy metal concentrations at 50 °C. (**d**) Cr(VI) under different initial heavy metal concentrations at 50 °C.

It is highly feasible to use transparent soil to simulate the migration of heavy metal pollutants in sandy soil. Specifically, for single heavy metal contaminants such as Cu(II) or Cr(VI), the concentration distribution fluctuation rate between transparent soil and sandy soil in both vertical and lateral migration directions is less than 10% (Figures 4 and 5). This indicates that transparent soil achieves over 90% accuracy in simulating the migration of a single heavy metal pollutant in sandy soil, demonstrating high reliability. In studies of composite heavy metal pollution, when the ratio of Cu(II) to Cr(VI) is 1:1, the concentration distribution fluctuation rate between transparent soil and sandy soil remains within 10% (Figures 6 and 7). This suggests that transparent soil can effectively simulate the migration behavior of these two heavy metals in sandy soil at the same proportion, with simulation accuracy exceeding 90%.

In summary, transparent soil serves as an effective medium for simulating the migration and transformation of heavy metal pollutants in sandy soil. Moreover, experimental observations indicate that both single pollutants and composite heavy metal pollutions exhibit differential sensitivities to factors such as temperature and initial concentration. To enhance future control measures for soil pollutants, it is imperative to investigate the impact of various conditions on the migration behavior of heavy metal pollutants.

3.2. Migration and Change in Transparent Soil Under Different Conditions

3.2.1. Effect of Dry Density on Migration Regularity

(1) Single heavy metal

Taking the effect of 1000 mg/kg at 60 °C as an example, the migration of a single heavy metal over time under different dry densities was analyzed (Figure 8a,b). As the experimental duration increased, the color interface of the heavy metal gradually moved upward. Under identical temperature and concentration conditions, higher dry density resulted in shorter migration distances for the heavy metals. This is attributed to the lower porosity and more tightly packed particles in high dry density soil, which increases resistance to water flow, thereby limiting the migration of heavy metals with water. Additionally, the change in the migration distance distribution curve for hexavalent chromium was observed to be smaller than that for copper ions (Cu^{2+}), indicating that dry density has a relatively minor impact on the migration of hexavalent chromium.

Figure 8c shows the migration rates of single heavy metal Cu(II) or Cr(VI) under different dry density conditions when the initial concentration is 1000 mg/kg. It can be observed that for Cu(II), pollutant mobility decreases with increasing soil dry density under the same conditions. When the heat source temperature surpasses 20 °C, the migration rate of Cr(VI) reaches its peak at a dry density of 1.4 g/cm^3, with a maximum mobility of 34.73%. However, the migration rate at a dry density of 1.5 g/cm^3 is always lower than that at a dry density of 1.3 g/cm^3. On the whole, it is roughly in line with the trend that the dry density of the soil increases and the migration rate changes inversely.

(2) Composite heavy metal

Taking the initial concentration of 1000 mg/kg and the heat source temperature of 60 °C as an example, the migration behavior of composite heavy metals was analyzed under different dry density conditions (Figure 9). The prominence of blue-green is not observed in transparent soil. Currently, only the distribution of orange-yellow for the two heavy metals can be seen. As the dry density of the soil increases, the proportion of the orange-yellow area decreases gradually. Notably, at a dry density of 1.5 g/cm^3 and a Cu(II) to Cr(VI) ratio of 1:1, an intense orange-red color interface is observed. This phenomenon indicates that the migration of heavy metal pollutants is characterized by a slow rate when the dry density of composite heavy metals reaches 1.5 mg/kg.

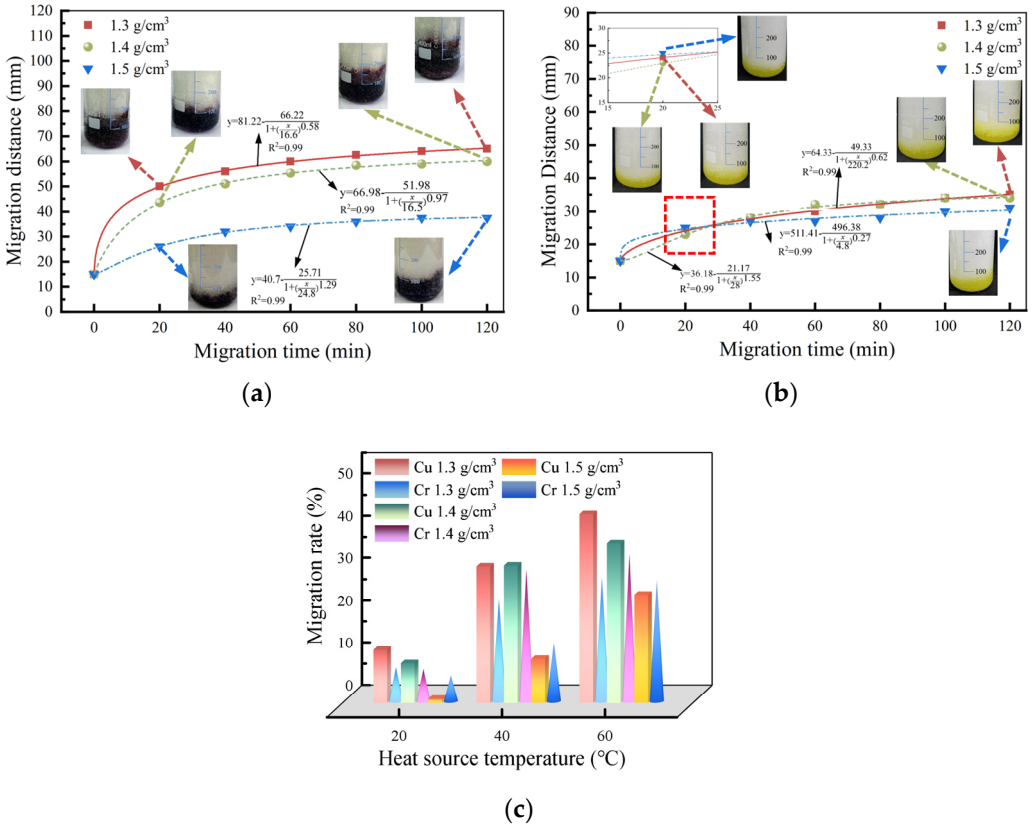

Figure 8. Migration effect of single Cu(II) or Cr(VI) under different dry densities. (**a**) Comparison of Cu(II) migration distances. (**b**) Comparison of Cr(VI) migration distances. (**c**) Migration rates of single heavy metal under different dry densities.

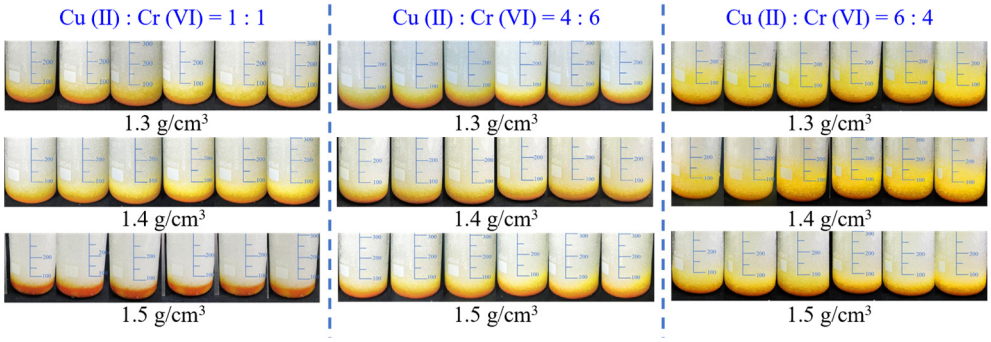

Figure 9. Interface distribution of different dry densities (interface distribution of six soil columns in each group was as follows: 20, 40, 60, 80, 100, and 120 min from left to right).

The migration effect of composite heavy metals under different dry densities when the initial concentration is 1000 mg/kg is illustrated in Figure 10. The migration of Cr(VI) in the 1:1 pollutant composition is more significant than that of Cu(II) under temperature field effect. This may be attributed to the high migration capacity and hydrophilicity of Cr(VI), which facilitates its spread and movement in soil. On the other hand, Cu(II) may be constrained by certain factors, resulting in a relatively lower degree of migration. Additionally, under this composite condition, both Cu(II) and Cr(VI) exhibit reduced mobility as soil dry density increases gradually. When the heat source temperature is 20 °C, heavy metal pollutant migration rate shows minimal fluctuations. Compared to other heavy metal complex conditions, dry density has little effect on the migration of 1:1 composite heavy metals.

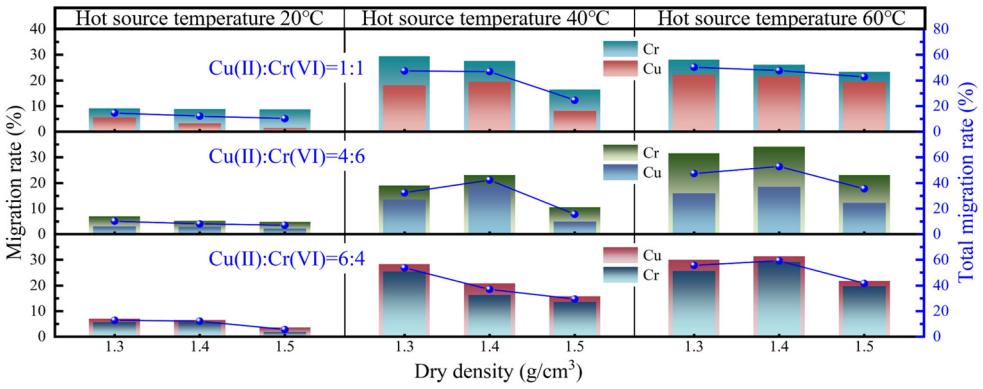

Figure 10. Migration effect of composite heavy metals under different dry densities.

3.2.2. Effect of Heat Source Temperature on Migration Rule

(1) Single heavy metal

Taking the dry density of 1.3 g/cm^3 and an initial heavy metal concentration of 500 mg/kg as an example, this study investigates the migration of single heavy metals under different heat source temperatures (Figure 11a,b). The results show that the migration distance of heavy metals increases gradually with rising heat source temperature. Specifically, for Cu(II) pollutants, significant migration toward the lower temperature end is observed at heat source temperatures of 40 °C and 60 °C. In contrast, for Cr(VI), significant migration toward the lower temperature end only occurs at a heat source temperature of 60 °C, which enhances the migration distance.

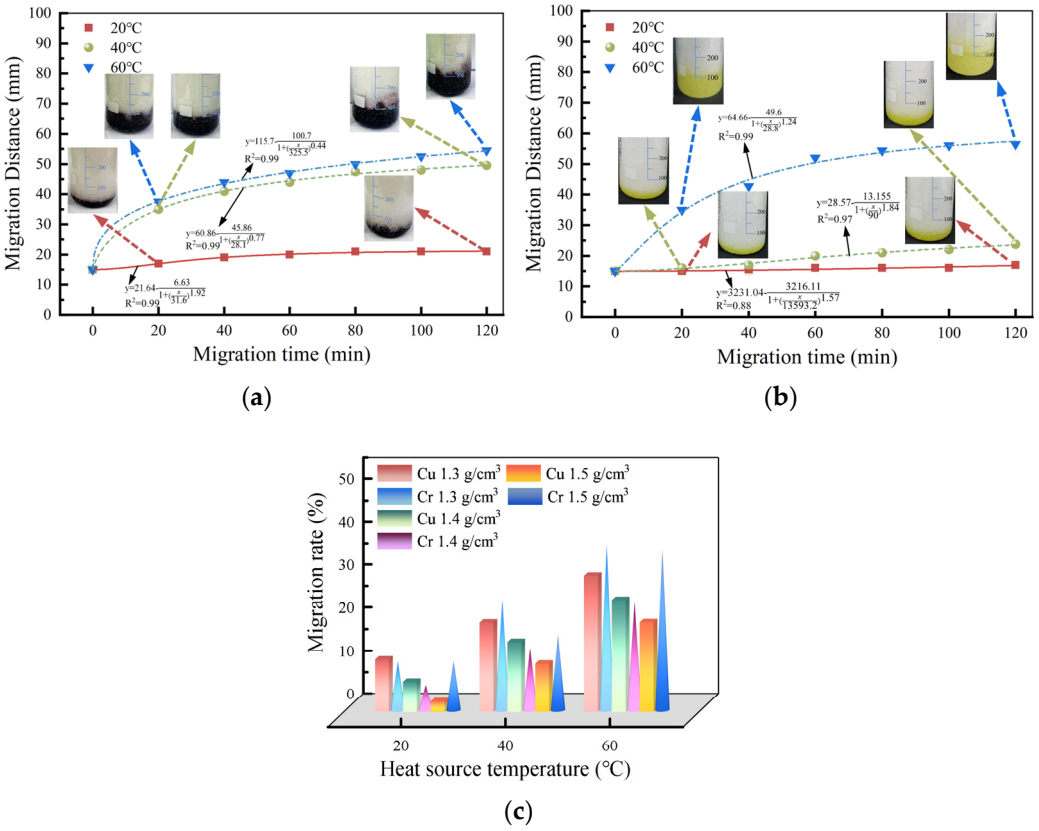

Figure 11. Migration effect of single Cu(II) or Cr(VI) at different heat source temperatures. (**a**) Comparison of Cu(II) migration distances. (**b**) Comparison of Cr(VI) migration distances. (**c**) Migration rates of single heavy metal under different heat source temperatures.

Figure 11c demonstrate a positive correlation between temperature and the migration rates of Cu(II) or Cr(VI), suggesting that temperature exerts a significant influence on the mobility of heavy metals within soil. Combined with Figures 10 and 11, it is evident that both heat source temperature and dry density significantly impact the migration of single Cu(II). However, for a single Cr(VI), the influence of heat source temperature outweighs that of dry density.

(2) Composite heavy metal

Taking the dry density of 1.3 g/cm^3 and the initial concentration of 500 mg/kg as an example, the migration of composite heavy metals at different heat source temperatures was analyzed (Figure 12). It shows that the proportion of orange-yellow regions increases with increasing temperature. Compared to other groups, the absence of a significant temperature gradient at a heat source temperature of 20 °C resulted in an inconspicuous upward migration of Cu(II) and Cr(VI). When the heat source temperature is set to 60 °C, the proportion of the orange-yellow region in the sample reaches its maximum. At this time, there is a blurred and fluctuating color interface, yet the overall trend remains consistently upward.

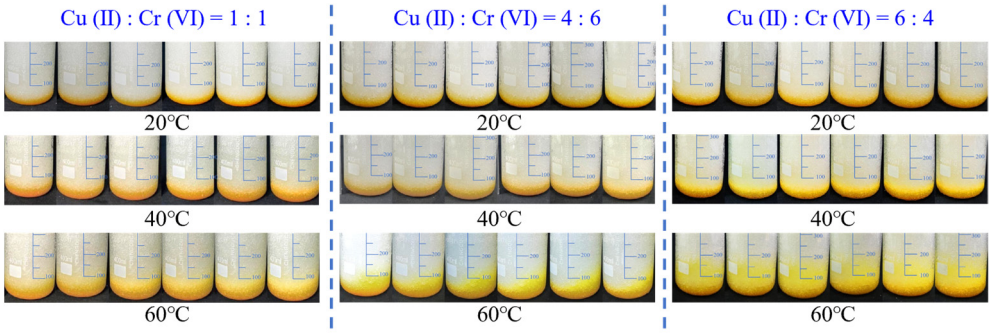

Figure 12. Temperature interface distributions of different heat sources.

The migration effect of composite heavy metals at different heat source temperatures is illustrated in Figure 13. The total migration rate and migration rate of composite heavy metals increase gradually with the rise in heat source temperature under identical conditions. In addition, the migration rate of Cr(VI) is observed to be higher than that of Cu(II) when the ratio between them is 1:1, suggesting that the migration of Cr(VI) is more influenced by temperature compared to Cu(II).

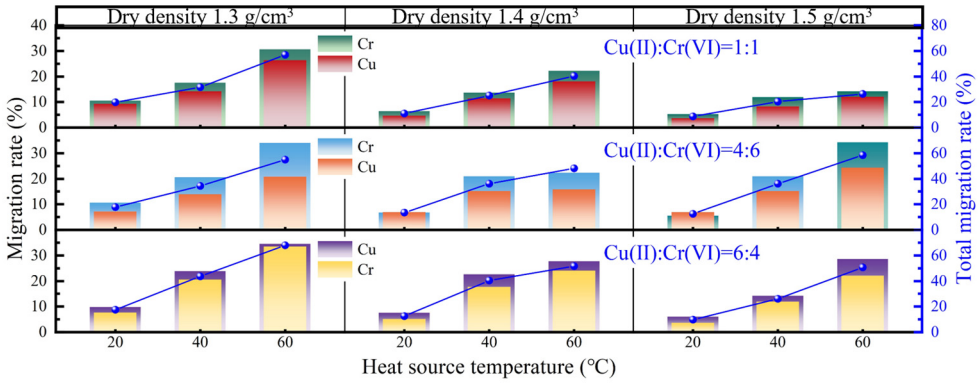

Figure 13. Migration effect of composite heavy metals at different heat source temperatures.

Combined with the changes in heavy metal migration at different temperatures, it is evident that a temperature gradient induces heat conduction and subsequent water migration within soil. Specifically, in regions of higher temperature, increased molecular activity facilitates the transfer of water from hotter to cooler areas, altering the spatial

distribution of soil moisture and promoting the migration of dissolved heavy metal ions. The long distance migration of heavy metal ions primarily occurs via two mechanisms: (1) convection, driven by directional flow; and (2) enhanced solubility and mobility of heavy metals due to temperature changes. Consequently, under a temperature gradient, the rate and extent of heavy metal ion migration significantly increases. In contrast, without a temperature gradient, soil moisture remains uniformly distributed, and there is no significant directional water movement. Therefore, in the management of heavy metal pollutants, controlling the migration range of heavy metals can be effectively achieved through temperature regulation.

3.2.3. Effect of Initial Heavy Metal Concentration on Migration Regularity

(1) Single heavy metal

Taking the dry density of 1.4 g/cm^3 and a heat source temperature of 60 °C as an example, the migration distances of single heavy metals under different initial concentrations were analyzed (Figure 14a,b). For Cu(II), the migration distance exhibits the most significant change when the initial concentration is 1000 mg/kg, and stabilizes once the migration distance reaches 60 mm. This indicates that both extremely low and high concentrations are not conducive to the migration of Cu(II) ions within soil. Conversely, for Cr(VI), higher initial concentrations lead to greater migration distances. This can be attributed to the enhanced molecular diffusion and combined convection effects caused by higher concentrations, which facilitate significant migration. In conjunction with Figure 14c, it is evident that the initial concentration of heavy metals has a similar impact on both Cu(II) and Cr(VI), with optimal migration occurring at an initial concentration of approximately 1000 mg/kg.

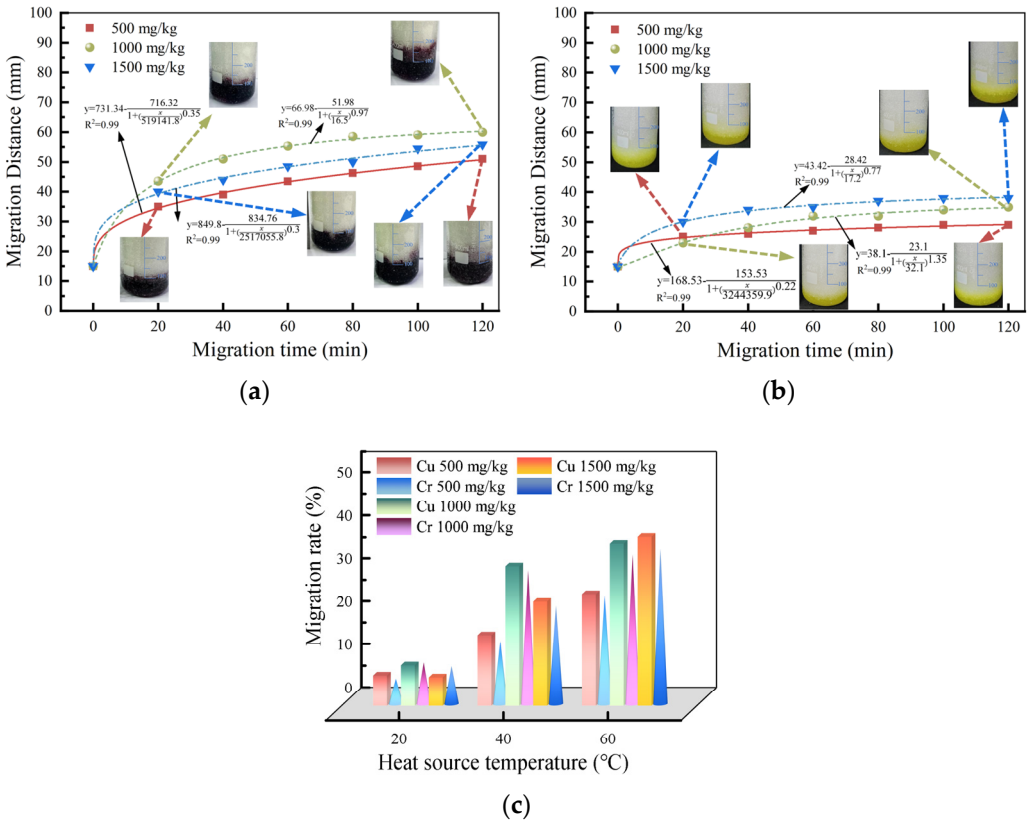

Figure 14. Migration effect of single Cu(II) or Cr(VI) at different heat source temperatures. (**a**) Comparison of Cu(II) migration distances. (**b**) Comparison of Cr(VI) migration distances. (**c**) Migration rates of single heavy metal under different initial concentrations.

(2) Composite heavy metal

Taking the dry density of 1.4 g/cm^3 and setting the heat source temperature at 60 °C as an example, the migration of complex heavy metals at different initial concentrations was analyzed (Figure 15). With increasing initial heavy metal concentration, the orange-yellow region deepened in color and its proportion gradually increased. When the initial concentration reached 1500 mg/kg, Cu(II) and Cr(VI) migrated against gravity toward the low temperature end, accompanied by a noticeable hydrodynamic dispersion effect. Consequently, there was a significant increase in the area of the color interface. This phenomenon was particularly pronounced when the ratio of Cu(II) to Cr(VI) reached 6:4.

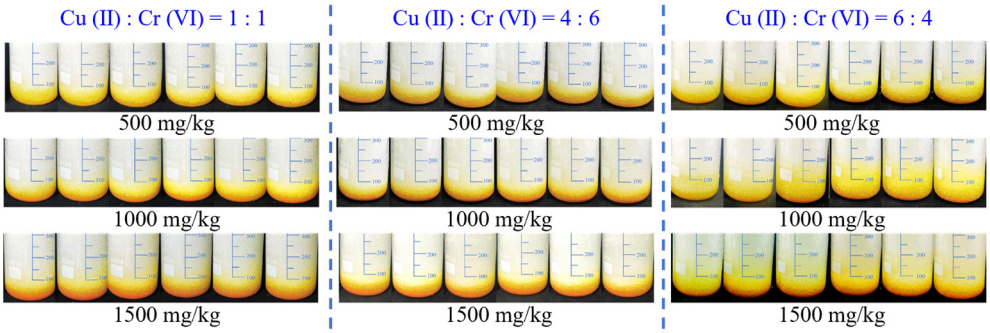

Figure 15. Interface distributions of different initial heavy metal concentrations.

The migration effect of composite heavy metals at different initial concentrations is presented in Figure 16. Under a constant heat source temperature of 20 °C, the migration rate remains relatively stable across different initial concentrations with an overall variation of less than 10%, suggesting minimal impact from concentration changes. However, when the temperature exceeds 20 °C, the total migration rate of Cu(II) and Cr(VI) at an initial concentration of 1500 mg/kg is lower compared to that at an initial concentration of 1000 mg/kg. Similarly, when the ratio between Cu(II) and Cr(VI) is set as 1:1, it can be observed that Cu(II)'s migration rate is weaker than that of Cr(VI).

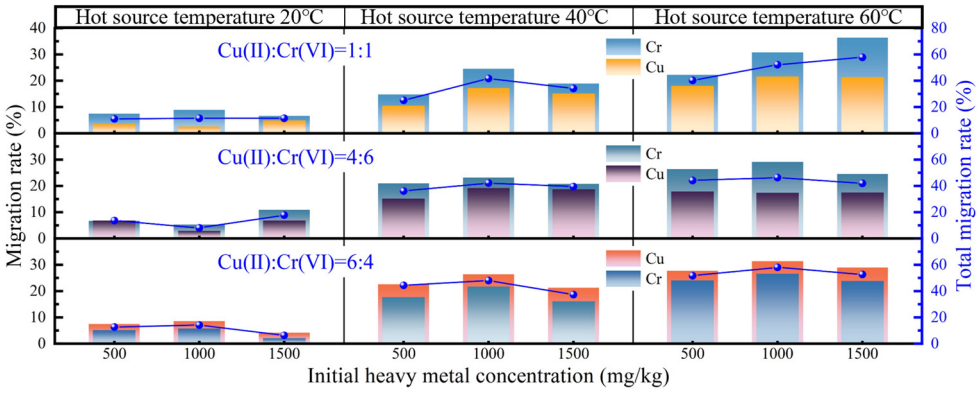

Figure 16. Migration effect of composite heavy metals at different initial concentrations.

In summary, dry density, heat source temperature, and initial concentration all exert significant influence on Cu(II)'s migration within single polluted transparent soil tests. For the single Cr(VI) pollutant, heat source temperature has a significant impact while dry density has a minor effect. The initial heavy metal concentration shows similar effects on both Cu(II) and Cr(VI), with good migration observed at an initial concentration of 1000 mg/kg. In composite-polluted transparent soil tests, the migration of heavy metals is primarily influenced by heat source temperature and initial heavy metal concentration rather than dry density. By precisely controlling the heating temperature and initial concentration of heavy metals, the treatment efficacy of heavy metal-contaminated soil can

be substantially enhanced. In practical applications, optimal regulation of these parameters not only improves remediation efficiency but also reduces energy consumption and cost.

3.3. Comparative Analysis of Occurrence Forms of Heavy Metal Pollutants

The distribution of heavy metal occurrence forms in soil is primarily influenced by the temperature of the heat source, compared to other factors. Therefore, we analyzed the occurrence forms of heavy metals under different heat source temperatures using a dry density of 1.3 g/cm^3 and initial concentration as an example. The proportion of EXC pollutants in the soil gradually increased with the rise in heat source temperature for Cu(II) in the four types of contaminated soil, while the proportions of Carb and RES states decreased progressively (Figure 17). This can be attributed to two main factors based on existing research and analysis [27,28]. Firstly, temperature influences porous media adsorption capacity, leading to decreased adsorption as temperature rises and the conversion of some stable RES states into EXC states. Secondly, elevated temperatures promote the hydrolysis of copper chloride solution, resulting in reduced pH values within the soil environment. Consequently, heavy metal Carb states most affected by changes in soil conditions are released into the environment [29]. The FeMnOx state and OM state of the remaining pollutants exhibit relatively high stability. Among these, the OM state accounts for a minute proportion, with a maximum value not exceeding 5.69%. This can be attributed to the absence of organic matter in transparent soil that could form ligands with metals present in the soil. Under varying heat source temperatures, the relative proportions of Cu(II) Carb states in different types of polluted soils are ranked as follows: 4:6 > 1:1 > 6:4 > single. The mobility of Cu(II) is observed to be directly proportional to the temperature change in the heat source, as evidenced by Figure 17c. Furthermore, this relationship is intricately linked with variations in both the EXC state and Carb state.

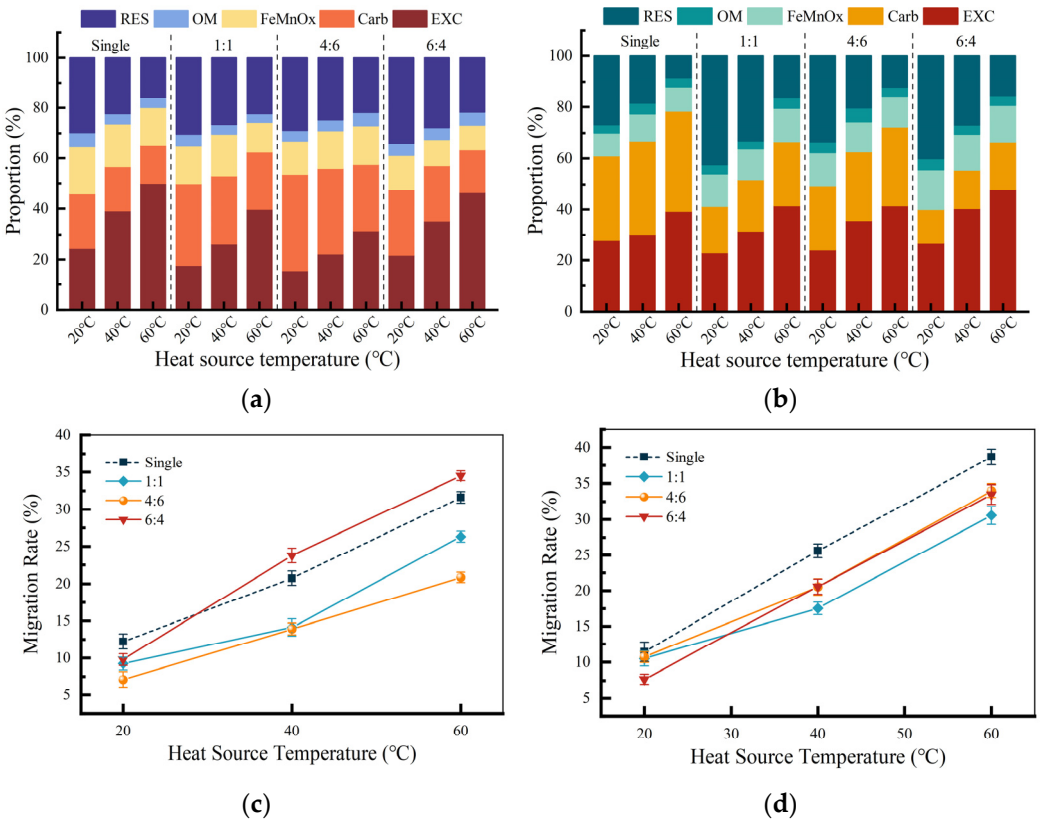

Figure 17. Occurrence forms and migration rates of Cu(II) and Cr(VI) in soils with different pollution types. (**a**) Cu(II)'s occurrence form. (**b**) Cr(VI)'s occurrence form. (**c**) Cu(II)'s migration rates. (**d**) Cr(VI)'s migration rates.

The results depicted in Figure 17 demonstrate that for Cr(VI), the proportion of the EXC state and Carb state gradually increases with the rise in heat source temperature across all four types of contaminated soil, while the proportion of the RES state decreases correspondingly. Notably, this trend is contrary to that observed for Cu(II). Primarily due to the weak acidity of chromic acid, an increase in temperature leads to a rise in soil ambient pH value, consequently resulting in an elevation of the proportion of the Carb state that exhibits high sensitivity toward changes in pH value. Under the influence of the temperature of each heat source, the proportion of the Carb states of Cr(VI) in different types of contaminated soils was ranked as follows: single > 4:6 > 1:1 > 6:4. The composite ratio of Cu(II) and Cr(VI) varies, leading to distinct pH values in the soil environment. Consequently, the proportion of the Carb states in their respective soils also differs. The migration rate of Cr(VI) in various polluted soils increases with the rise in temperature gradient, as evidenced by the combination of Figure 17d. This phenomenon is attributed to the escalating proportion of the EXC and Carb states.

3.4. Comparison and Discussion

Transparent soil is extensively utilized in geotechnical engineering simulations owing to its exceptional transparency, controllable physical properties, and stable chemical characteristics. For instance, this method can simulate soil mechanics, enabling the observation of soil deformation and crack formation, thereby facilitating the prevention and mitigation of geological disasters. Moreover, it can support underground engineering simulations, such as observing soil deformation during subway tunnel construction, which aids in evaluating project safety and stability. Furthermore, transparent soil can be applied to soil and water engineering simulations, allowing for the analysis of levee channel structures and predicting strength, stability, and flow changes during engineering operations. Existing studies have shown that transparent soil technology meets the research requirements for investigating the internal structure and dynamic behavior of geotechnical materials, providing clear a visualization of deformation, flow, and other physical processes within soil [30,31].

Understanding the migration of heavy metal pollutants in soil is crucial for pollution control, environmental protection, and safeguarding human health. In recent years, as concerns about environmental pollution have grown, scientists have been developing innovative methods to investigate the migration behavior of heavy metals in soil. This study introduces the concept of transparent soil into the field of heavy metal-contaminated soil research, aiming to explore the migration patterns of heavy metals through the integration of visualization and color rendering technologies. As shown in Table 1, the density, particle size, saturated water content, and other characteristics of the transparent soil described herein closely resemble those of medium sand and fine sand, in accordance with the standard for engineering classification of soil [32] (GB/T 50145-2007). This makes transparent soil an ideal substitute material for studying heavy metal migration. To validate the effectiveness of transparent soil, we conducted several experiments comparing the two-dimensional interface migration data of transparent soil and sandy soil under various influencing factors (see Figures 3–6). The results demonstrated that the performance of both materials in heavy metal migration was highly consistent, further confirming the suitability and effectiveness of transparent soil for investigating heavy metal migration dynamics in contaminated soil.

Compared with traditional laboratory detection methods, transparent soil technology exhibits significant advantages in the study of heavy metal migration. Firstly, the transparent soil model maintains the original integrity of the soil by eliminating the need for embedded sensors, thereby minimizing structural alterations and preserving natural

conditions. Secondly, compared to X-ray technology, transparent soil technology is not only more cost-effective but also simpler to operate, allowing for the real-time observation of pollutant migration processes. This direct visualization provides researchers with a powerful tool to better understand the mechanisms of heavy metal migration in soil. Additionally, transparent soil technology offers greater potential for future research. For instance, by adjusting the composition and structure of transparent soils to simulate various types of soil environments, researchers can gain deeper insights into the migration behavior of heavy metals under different conditions. In summary, transparent soil technology offers a novel perspective and methodology for investigating heavy metal migration in soil, demonstrating broad application potential. This innovative approach enables scientists to more precisely evaluate the risks associated with heavy metal contamination, thereby providing a robust scientific foundation for the formulation of effective pollution mitigation strategies. Table 3 provides a detailed comparison of the advantages and limitations of transparent soil technology relative to traditional methods, further highlighting its distinctive benefits.

Table 3. Comparison of transparent soil technique versus traditional methods.

Method	Type					
	Interference	**Visualization**	**Visibility**	**Accuracy**	**Easy Operating**	**Economy**
Leaching [33]	√	×	×	×	×	×
Transparent soil [34]	×	√	√	√	√	√
X-ray techniques [35]	×	×	√	×	×	×
Software simulation [36]	×	×	×	×	√	√
Carbon quantum dot detection [37]	√	×	√	√	×	×

Note: "√" indicates the presence of a feature, while "×" denotes its absence.

However, for the theoretical research of pollutant migration simulation based on transparent soil, it is crucial to develop more precise index testing methods to ensure the reproducibility and reliability of the experimental results. Integrating advanced image acquisition technology with machine learning processing represents a significant development trend in this field. Utilizing high-precision cameras and sensors enables real-time recording of pollutant diffusion in transparent soil, generating substantial amounts of high-quality image data. These images can subsequently be processed and analyzed by machine learning algorithms to automatically identify contaminant distribution patterns, migration pathways, and interactions with other substances. This approach not only enhances the speed and accuracy of data analysis but also minimizes errors associated with manual intervention. Furthermore, the application of digitalization and automation technologies facilitates comprehensive monitoring and management of the entire experimental process. In summary, combining more accurate indicator test methods with advanced image acquisition and machine learning technologies in the simulation of pollutant migration based on transparent soil will significantly advance this field and provide a more scientific and reliable foundation for environmental protection and pollution control.

4. Conclusions

Through the investigation of heavy metal pollutant migration and diffusion in porous media using transparent soil, the following conclusions can be inferred:

1. Under identical conditions of porous media parameters, the concentration fluctuation rate of heavy metal pollutants in the simulated sandy soil of the experimental group is less than 10%, indicating a simulation accuracy exceeding 90%. Consequently, it is

feasible to employ transparent soil as a medium for visually monitoring the migration and diffusion processes of heavy metal pollutants in sandy soil.

2. In the single-contaminated transparent soil test, the migration of Cu(II) pollutants is significantly influenced by dry density, heat source temperature, and initial heavy metal concentration. For Cr(VI), the effect of heat source temperature is significant, while the effect of the initial concentration is similar to that of Cu(II). In the combined pollution transparent soil test, heavy metal migration primarily depends on heat source temperature and the initial heavy metal concentration, with less impact from dry density.
3. The proportion of the Cu(II) Carb state in different types of polluted soil under temperature field is as follows: 4:6 > 1:1 > 6:4 > single; while the proportion of Cr(VI) Carb state is as follows: single > 4:6 > 1:1 > 6:4. The variation in the pH value within the soil environment influences the transformation of heavy metal carbonate binding states.

Author Contributions: Methodology, Z.Q.; software, C.Z.; validation, C.Z., H.Y. and Z.Q.; formal analysis, C.Z.; investigation, H.Y.; resources, M.L.; data curation, H.Y.; writing—original draft preparation, Z.Q.; writing—review and editing, C.Z.; visualization, C.Z.; supervision, M.L.; funding acquisition, M.L. All authors have read and agreed to the published version of the manuscript.

Funding: The authors are grateful for the financial support from the National Natural Science Foundation of China (Project nos. 51978235 and 52278341), and the Natural Science Foundation of Hebei (Project no. E2023202087).

Data Availability Statement: The data supporting the findings of this study can be obtained from the corresponding author upon request.

Conflicts of Interest: The authors declare no conflict of interest.

References

1. He, L.Z.; Zhong, H.; Liu, G.X.; Dai, Z.M.; Brookes, P.C.; Xu, J. Remediation of Heavy Metal Contaminated Soils by Biochar: Mechanisms, Potential Risks and Applications in China. *Environ. Pollut.* **2019**, *252*, 846–855. [CrossRef]
2. He, P.L.; Guo, J.J.; Zhang, S.X. Feasibility of Microbially Induced Carbonate Precipitation to Enhance the Internal Stability of Loess under Zn-Contaminated Seepage Conditions. *Buildings* **2024**, *14*, 1230. [CrossRef]
3. Xiang, M.T.; Li, Y.; Yang, J.Y.; Lei, K.G.; Li, Y.; Li, F.; Zheng, D.F.; Fang, X.Q.; Cao, Y. Heavy Metal Contamination Risk Assessment and Correlation Analysis of Heavy Metal Contents in Soil and Crops. *Environ. Pollut.* **2021**, *278*, 116911. [CrossRef]
4. Wu, Y.D.; Ren, J.C.; Liu, J. Field Investigation of Water Infiltration into a Three-Layer Capillary Barrier Landfill Cover System Using Local Soils and Construction Waste. *Buildings* **2024**, *14*, 139. [CrossRef]
5. Rahman, Z.; Singh, V.P. The Relative Impact of Toxic Heavy Metals (Thms) (Arsenic (as), Cadmium (Cd), Chromium (Cr)(Vi), Mercury (Hg), and Lead (Pb)) on the Total Environment: An Overview. *Environ. Monit. Assess.* **2019**, *191*, 419. [CrossRef] [PubMed]
6. Tang, J.Y.; Zhang, J.C.; Ren, L.H.; Zhou, Y.Y.; Gao, J.; Luo, L.; Yang, Y.; Peng, Q.H.; Huang, H.L.; Chen, A.W. Diagnosis of Soil Contamination Using Microbiological Indices: A Review on Heavy Metal Pollution. *J. Environ. Manag.* **2019**, *242*, 121–130. [CrossRef] [PubMed]
7. Vareda, J.P.; Valente, A.J.M.; Duraes, L. Assessment of Heavy Metal Pollution from Anthropogenic Activities and Remediation Strategies: A Review. *J. Environ. Manag.* **2019**, *246*, 101–118. [CrossRef] [PubMed]
8. Qin, G.W.; Niu, Z.D.; Yu, J.D.; Li, Z.H.; Ma, J.Y.; Xiang, P. Soil Heavy Metal Pollution and Food Safety in China: Effects, Sources and Removing Technology. *Chemosphere* **2021**, *267*, 129205. [CrossRef] [PubMed]
9. Rajendran, S.; Priya, T.A.K.; Khoo, K.S.; Hoang, T.K.A.; Ng, H.S.; Munawaroh, H.S.H.; Karaman, C.; Orooji, Y.; Show, P.L. A Critical Review on Various Remediation Approaches for Heavy Metal Contaminants Removal from Contaminated Soils. *Chemosphere* **2022**, *287*, 132369. [CrossRef] [PubMed]
10. Sall, M.L.; Diaw, A.K.D.; Gningue-Sall, D.; Aaron, S.E.; Aaron, J.J. Toxic Heavy Metals: Impact on the Environment and Human Health, and Treatment with Conducting Organic Polymers, a Review. *Environ. Sci. Pollut. Res.* **2020**, *27*, 29927–29942. [CrossRef]
11. Kumar, A.; Song, H.W.; Mishra, S.; Zhang, W.; Zhang, Y.L.; Zhang, Q.R.; Yu, Z.G. Application of Microbial-Induced Carbonate Precipitation (Micp) Techniques to Remove Heavy Metal in the Natural Environment: A Critical Review. *Chemosphere* **2023**, *318*, 137894. [CrossRef] [PubMed]
12. Nartowska, E.; Podlasek, A.; Vaverkova, M.D.; Koda, E.; Jakimiuk, A.; Kowalik, R.; Kozlowski, T. Mobility of Zn and Cu in Bentonites: Implications for Environmental Remediation. *Materials* **2024**, *17*, 2957. [CrossRef] [PubMed]

13. Wang, Y.; Gu, K.; Wang, H.S.; Shi, B.; Tang, C.S. Remediation of Heavy-Metal-Contaminated Soils by Biochar: A Review. *Environ. Geotech.* **2022**, *9*, 135–148. [CrossRef]
14. Rehman, Z.; Junaid, M.F.; Ijaz, N.; Khalid, U.; Ijaz, Z. Remediation Methods of Heavy Metal Contaminated Soils from Environmental and Geotechnical Standpoints. *Sci. Total Environ.* **2023**, *867*, 161468. [CrossRef] [PubMed]
15. Ni, Q.C.; Hird, C.C.; Guymer, I. Physical Modelling of Pile Penetration in Clay Using Transparent Soil and Particle Image Velocimetry. *Geotechnique* **2010**, *60*, 121–132. [CrossRef]
16. Xu, D.; Lei, H.; Wuxing, W.; Jian, C. Visualization Experiment Technology Based on Transparent Geotechnical Materials and Its Engineering Application. *J. Vis.* **2023**, *26*, 145–159.
17. Ding, X.; Wu, Q.; Huang, Y.; Zhang, Y. Model Test on the Soil Arching Effect of Pile-Supported Embankments Using Transparent Soil. *Geotech. Test. J.* **2021**, *44*, 20190347. [CrossRef]
18. Zhou, C.; Ma, W.; Sui, W. Transparent Soil Model Test of a Landslide with Umbrella-Shaped Anchors and Different Slope Angles in Response to Rapid Drawdown. *Eng. Geol.* **2022**, *307*, 106765. [CrossRef]
19. Yuan, B.X.; Sun, M.; Xiong, L.; Luo, Q.Z.; Pradhan, S.P.; Li, H.Z. Investigation of 3d Deformation of Transparent Soil around a Laterally Loaded Pile Based on a Hydraulic Gradient Model Test. *J. Build. Eng.* **2020**, *28*, 101024. [CrossRef]
20. He, C.Q.; Hu, A.N.; Wang, F.F.; Zhang, P.; Zhao, Z.Z.; Zhao, Y.P.; Liu, X.Y. Effective Remediation of Cadmium and Zinc Co-Contaminated Soil by Electrokinetic-Permeable Reactive Barrier with a Pretreatment of Complexing Agent and Microorganism. *Chem. Eng. J.* **2021**, *407*, 126923. [CrossRef]
21. Goswami, A.P.; Das, S.; Kalamdhad, A.S. Monitoring and Risk Assessment of Heavy Metals Surficial Sediments Using the 5-Step Sequential Extraction Process. *Int. J. Environ. Anal. Chem.* **2021**, *103*, 7519–7540. [CrossRef]
22. Hegedűs, M.; Tóth-Bodrogi, E.; Németh, S.; Somlai, J.; Kovács, T. Radiological Investigation of Phosphate Fertilizers: Leaching Studies. *J. Environ. Radioact.* **2017**, *173*, 34–43. [CrossRef] [PubMed]
23. Liu, J.Y.; Iskander, M.G. Modelling Capacity of Transparent Soil. *Can. Geotech. J.* **2010**, *47*, 451–460. [CrossRef]
24. Ganiyu Abideen, A.; Rashid Ahmad Safuan, A.; Osman Mohd, H. Utilisation of Transparent Synthetic Soil Surrogates in Geotechnical Physical Models: A Review. *J. Rock Mech. Geotech. Eng.* **2016**, *8*, 568–576. [CrossRef]
25. Tessier, A.P.; Campbell, P.G.C.; Bisson, M.X. Sequential Extraction Procedure for the Speciation of Particulate Trace Metals. *Anal. Chem.* **1979**, *51*, 844–851. [CrossRef]
26. Rauret, G.; Rubio, R.; Lopez-Sanchez, J.F. Optimization of Tessier Procedure for Metal Solid Speciation in River Sediments. *Int. J. Environ. Anal. Chem.* **1989**, *36*, 69–83. [CrossRef]
27. Huang, H.J.; Yuan, X.Z. The Migration and Transformation Behaviors of Heavy Metals During the Hydrothermal Treatment of Sewage Sludge. *Bioresour. Technol.* **2016**, *200*, 991–998. [CrossRef]
28. Li, Q.; Wang, Y.H.; Li, Y.C.; Li, L.F.; Tang, M.D.; Hu, W.F.; Chen, L.; Ai, S.Y. Speciation of Heavy Metals in Soils and Their Immobilization at Micro-Scale Interfaces among Diverse Soil Components. *Sci. Total Environ.* **2022**, *825*, 153862. [CrossRef]
29. Bastami, K.D.; Neyestani, M.R.; Esmaeilzadeh, M.; Haghparast, S.; Alavi, C.; Fathi, S.; Nourbakhsh, S.; Shirzadi, E.A.; Parhizgar, R. Geochemical Speciation, Bioavailability and Source Identification of Selected Metals in Surface Sediments of the Southern Caspian Sea. *Mar. Pollut. Bull.* **2017**, *114*, 1014–1023. [CrossRef]
30. Yang, M.H.; Xiao, J.X.; Yang, T. Comparative Experimental Study on Deformation of Transparent Soil Induced by Construction of Quasi-rectangular and Circular Tunnels at Different Buried Depths. *J. Hunan Univ. (Nat. Sci.)* **2024**, *51*, 66–75.
31. Wang, Y.C.; Fang, X.W.; Wang, L.Q. The Effect of Water Level Fluctuation Rate on Reservoir Landslides by Transparent Soil Model Experimental Study. *J. Civ. Environ. Eng.* **2024**, 1–10.
32. *GB/T 50145-2007*; Domestic-National Standard-China State Administration for Market Regulation CN-GB. Standard for Engineering Clas-sification of Soil. China Plan Publishing House: Beijing, China, 2007.
33. Sun, R.G.; Gao, Y.; Yang, Y. Leaching of Heavy Metals from Lead-Zinc Mine Tailings and the Subsequent Migration and Transformation Characteristics in Paddy Soil. *Chemosphere* **2022**, *291*, 9–25. [CrossRef]
34. Zhang, W.A.; Gu, X.; Zhong, W.H.; Ma, Z.T.; Ding, X.M. Review of Transparent Soil Model Testing Technique for Underground Construction: Ground Visualization and Result Digitalization. *Undergr. Space* **2022**, *7*, 702–723. [CrossRef]
35. Bornert, M.; Lenoir, N.; Bésuelle, P.; Pannier, Y.; Hall, S.A.; Viggiani, G. Discrete and Continuum Analysis of Localised Deformation in Sand Using X-ray μCT and Volumetric Digital Image Correlation. *Géotechnique* **2010**, *60*, 11–20.
36. Wang, Z.; Gu, X.; Xie, T.; Xu, X. Simulation of Heavy Metal Pollutants Migration in Soil Based on Finite Volume Method. *J. Northeast. Univ. Nat. Sci.* **2018**, *39*, 867–871.
37. Liu, S.Y.; Wu, Z.T.; Nian, N.J.; Zhang, P.; Ni, L. The Speciation of Heavy Metal Chromium in Water Environment by Carbon Quantum Dots System. *Water Air Soil Pollut.* **2024**, *235*, 9–26. [CrossRef]